LA-UR- 99-2245

Approved for public release; distribution is unlimited.

Title: Texture and Yield Stress of Pre-Strained 304L Stainless Steel

Author(s): Kristin Bennett, LANSCE-12
Bob Von Dreele, LANSCE-12
G. T. Gray, III, MST-8
S. R. Chen, MST-8

Submitted to: Proceedings of The Neutron Texture and Stress Analysis Conference
Dubna Russia
June 23-26, 1997

RECEIVED
SEP 07 1999
OSTI

Los Alamos
NATIONAL LABORATORY

Los Alamos National Laboratory, an affirmative action/equal opportunity employer, is operated by the University of California for the U.S. Department of Energy under contract W-7405-ENG-36. By acceptance of this article, the publisher recognizes that the U.S. Government retains a nonexclusive, royalty-free license to publish or reproduce the published form of this contribution, or to allow others to do so, for U.S. Government purposes. Los Alamos National Laboratory requests that the publisher identify this article as work performed under the auspices of the U.S. Department of Energy. Los Alamos National Laboratory strongly supports academic freedom and a researcher's right to publish; as an institution, however, the Laboratory does not endorse the viewpoint of a publication or guarantee its technical correctness.

DISCLAIMER

This report was prepared as an account of work sponsored by an agency of the United States Government. Neither the United States Government nor any agency thereof, nor any of their employees, make any warranty, express or implied, or assumes any legal liability or responsibility for the accuracy, completeness, or usefulness of any information, apparatus, product, or process disclosed, or represents that its use would not infringe privately owned rights. Reference herein to any specific commercial product, process, or service by trade name, trademark, manufacturer, or otherwise does not necessarily constitute or imply its endorsement, recommendation, or favoring by the United States Government or any agency thereof. The views and opinions of authors expressed herein do not necessarily state or reflect those of the United States Government or any agency thereof.

DISCLAIMER

Portions of this document may be illegible in electronic image products. Images are produced from the best available original document.

Paper to be submitted to:
Proceedings of the Neutron Texture and Stress Analysis Conference, June 23-26, 1997
at the JINR-Dubna, Russia

Texture and yield stress of pre-strained 304L stainless steel

Authors:
K. Bennett, R. B. Von Dreele, G. T. Gray III, and S. R. Chen
Los Alamos National Laboratory, Los Alamos, NM 87545 USA

The evolution of texture and yield stress in 304L stainless steel is investigated as a function of deformation to large plastic strains. Steel bars quasi-statically upset forged at a strain rate of $0.001s^{-1}$ to true strains of 0, 0.5, 1.0 and 1.8 were found to acquire their texture (~3.0 m.r.d.) in the first 0.5 strain with (110) poles highly aligned parallel to the compression direction independent of whether the pre-forged starting material was in a cold worked or annealed (1050°C for 1 hour) condition. The same bars, when strained at room temperature show an incremental yield with pre-strain regardless of strain rate (10^{-1} or $10^{-3}s^{-1}$) or thermal history, though annealed bars yield at slightly lower stresses. At 77 K and strain rate $10^{-3}s^{-1}$, the annealed 304L exhibits more pronounced strain-hardening behavior than the 304L forged in a cold-worked condition.

Introduction

Texture and stress-strain behavior are two important probes that are used to characterize as well as form the basis of physically-based material models used to predict plastic flow in polycrystalline metals. Many metals whether cold worked or annealed, are ductile when subjected to fabrication processes such as extrusion, rolling, forming or forging. In this study we use texture and compressive stress-strain behavior to track the structural evolution in 304L stainless steel as it undergoes increasing plastic deformation to large strains.

The mechanical behavior of 304L stainless steel is a material that has a range of United Sates Department of Energy (DOE) weapons applications. Its high elastic modulus, modulus-to-density, and strength-to-density ratio make it an ideal material for aerospace vehicles and weapons components. The success of its application depends on an accurate description of the microstructure of the material as a function of various fabrication, forming or dynamic histories. Structural parameters such as texture and yield stress are critical for its application and for predictive capability. Structural properties such as strain rate sensitivity, strain hardening and yield locus in 304L stainless steel have already been measured and modeled for various forming and impact problems to create a data base for prediction of its constitutive properties [1].

To measure the texture data in this study we used a novel application of Rietveld refinement and neutron Time-of-Flight (TOF) diffraction [2]. Even order Orientation Distribution Function (ODF) harmonic coefficients up to the 14^{th} degree are extracted

from a combination of 50-60 TOF neutron diffraction spectra. We do not calculate the ODF directly from the harmonic coefficients because we only have the even order coefficients from the diffraction patterns. From the even order coefficients we extract the traditional two-dimensional pole figure. While this method differs from the usual technique of measuring 3-4 individual pole figures of selected hkl reflections, the Rietveld calculations have proved to be highly successful and reproducible [3-5] and are the most efficient use of TOF diffraction. When textures are weak and harmonic orders are relatively low, we find secondary artifacts from our "two-step" calculation procedure minimal. Furthermore, neutron diffraction offers the important advantage of low absorption so that bulk samples (1-2 cm^3) can be investigated [6]. To characterize stress-strain behavior in this study, we used the traditional method of measuring compressive stress/strain-curves at both quasi-static and dynamic strain rates. An Instron testing machine was used to perform compression tests at strain rates of 0.001 and 0.1 s^{-1}. A Split-Hopkinson Pressure Bar (SHPB) was used to perform the dynamic tests where stress is proportional to the amplitude of the transmitted wave and strain is proportional to the reflected wave [7].

Experiments

The material used in this study was austenitic 304L stainless steel (obtained in 4.45 cm-dia. bar form which was redrawn from 15.2 cm-dia. bar stock) containing the major elements, Cr (18.5%), Ni (11.4%), Mn (1.8%) with a δ–ferrite phase (<0.6%). Half of the stock was upset forged in the cold-worked state (grain size = 100-200 μm) while the remaining half was annealed at 1050°C for 1 hour in vacuum (grain size = 10-50 μm) prior to forging. Each material was quasi-statically upset-forged at a strain rate of 0.001 s^{-1} to true strains of ε=0, 0.5, 1.0, 1.8. Samples sectioned from the upset-forged bars were characterized to study their texture evolution in addition to their flow-stress responses as a function of forging strain and the starting microstructural condition of the 304L.

For the texture measurements, complete pole figures were determined by TOF neutron diffraction on the High Intensity Neutron Diffractometer (HIPD) at the Lujan Center, Los Alamos National Laboratory [8]. Samples (1 cm-dia. x 1 cm-long) were mounted on a two-circle Eulerian cradle capable of rotating a specimen 0-360 degrees in both the azimuthal (ω) and polar (χ) directions. Data from 4 detector banks for each of 13 orientation (ω–χ) settings, were combined to calculate the even order orientation distribution coefficients using a generalized spherical harmonics method and Rietveld refinement [5]. The maximum order of the spherical harmonic coefficients used was 14 with a total of 7 spherical harmonic terms. Complete pole figures were calculated from these spherical harmonic coefficients and input into POPLA [9] for generation of the ODF via WIMV [10] and for graphical display of the ODF. The same refinements used to determine harmonic coefficients were also used to calculate microstrains [11,12]. The evolution of texture and microstrain as a function of pre-strain for both the cold worked and annealed 304L bars were determined.

For the yield measurements, stress-strain curves revealing yield stresses were determined at quasi-static compression strains for both the cold worked and annealed samples at strain rates of .001 s^{-1} using a screw-driven Instron Testing Machine. 2 LVDT's mounted on the samples (.5 cm-dia. x .5 cm -long) recorded the true strains. Samples either cold worked or annealed, were prestrained (0, 0.5, 1.0, 1.8) and deformed at room temperature. A second and third set of annealed samples were tested at a rate of $0.1s^{-1}$ at room temperature and at a rate of $0.001s^{-1}$ at 77 K, respectively. Stress-strain curves were measured at dynamic strains using a Split-Hopkinson Pressure Bar (SHPB) [7,13]. Strain gauges on both incident and transmitted pressure bars (7.6 mm-long) on either side of the sample (.5 cm-dia. x .5 cm-long) record stress wave propagation and reflected waves which are integrated to ascertain stress and strain within the sample. One set of the forged cold-worked 304L steel was tested at strain rates of $2000s^{-1}$ and room temperature.

Texture Results and Discussion

The forged 304L stainless steels in this study were found to acquire their texture (~3 m.r.d.) in the first 0.5 strain with (110) poles highly aligned parallel to the direction of compression regardless of their preforging thermal history (Figure 1 & Figure 2). These results for 304L stainless steel are consistent with {111}<110> as the dominant slip mode found in most f.c.c. metals [14]. While all pole figures for samples pre-strained more than 0% describe a fiber texture with <110> as fiber axis, the textures are not true "simple" fiber textures where the axes are distributed equally about the fiber direction. The crystallographic poles for both the cold-worked and annealed steel samples show distinct maxima around the fiber axis that evolve with increasing pre-strain. At ε=0.5 the crystallographic poles of the cold-worked material distribute themselves orthotropically into 4 distinct maxima around the fiber axis while those of annealed-samples distribute into 6. However, with increasing pre-strain, these maxima disappear in both sets of samples. In the cold-worked material the maxima evolve from 4 to at ε= 1.0 and broaden and at ε=1.8 the maxima nearly disappear. In the annealed material the 6 maxima become 4 at ε=1.0 and completely disappear at ε=1.8.

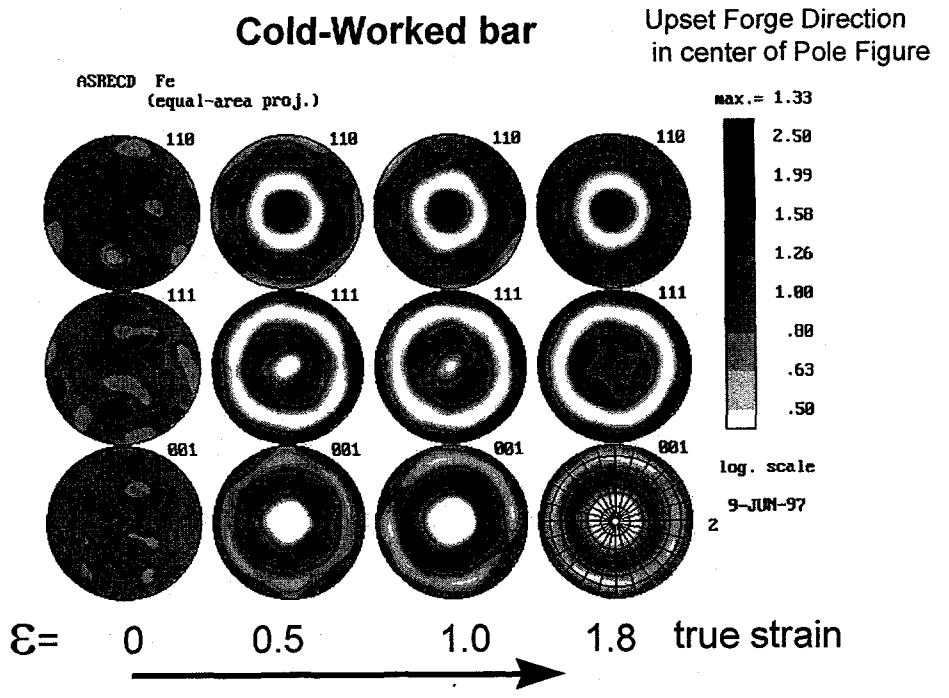

Figure 1. (110), (111), (001) pole figures for cold-worked 304L samples as a function of pre-strains (ε=0, 0.5, 1.0, 1.8) showing (110) aligned parallel to compression and 4 distinct maxima at ε=0.5, representing cyclic fiber texture. Pole figures are plotted in equal area projection with direction of compression in center. Densities expressed as multiple of random distribution (m.r.d.).

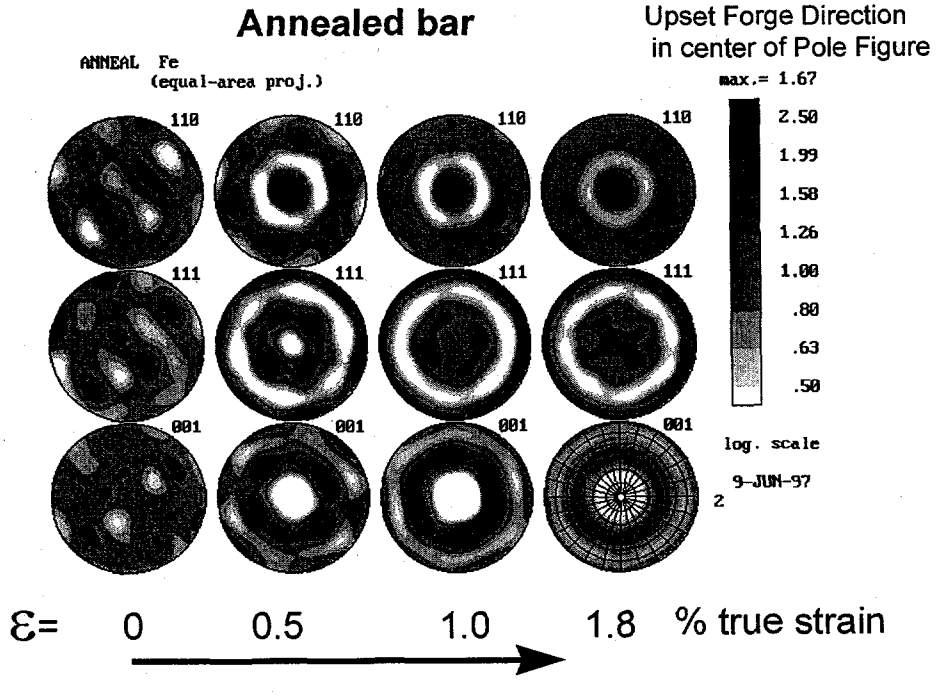

Figure 2. (110), (111), (001) pole figures for annealed 304L specimens as a function of pre-strains (ε=0, 0.5, 1.0, 1.8) showing (110) aligned parallel to compression and 6 distinct maxima at ε=0.5, representing cyclic fiber texture. Pole figures are plotted in equal area projection with direction of compression (upset-forging) in center. Densities expressed as multiple of random distribution (m.r.d.).

In many cases the expression of the texture by pole figures is an oversimplification of the texture and the texture is only adequately described by the complete ODF. The ODF predicts anisotropy of physical properties. As a way of enhancing the nature fiber texture and the deviation from a simple fiber texture, we plot the orientation distribution function in oblique sections in Figures 3 a & b. These sections are plotted at constant ν where ν is defined by the linear relationship $\nu=(\psi-\phi)/2$ in symmetric (Kocks) Euler angles. The deviation from simple fiber texture may be due to inhomogeneous strain across the radius of the sample related to microstructural banding. At ε=1.8 the non uniformity or cyclic texture may additionally be due to the presence of a small amount of δ-ferrite phase that is formed during a martensitic strain-induced transformation at high plastic strains. Furthermore these results are bulk measurements and the shear strain may change continuously from the surface to the center of the specimen.

a

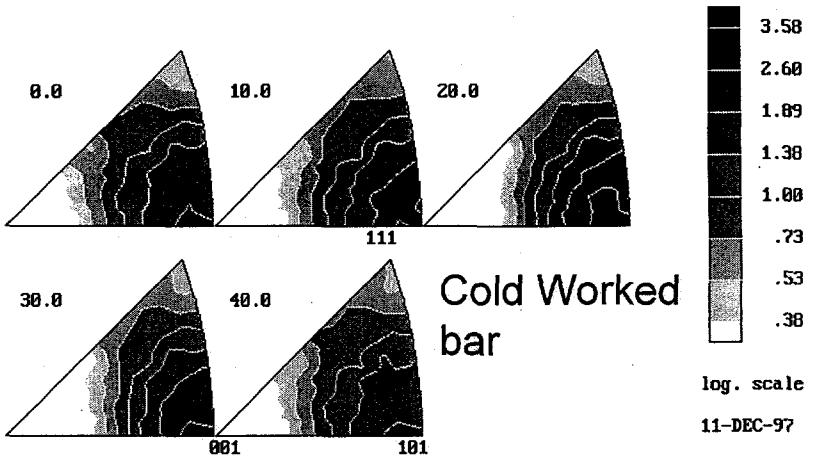

b

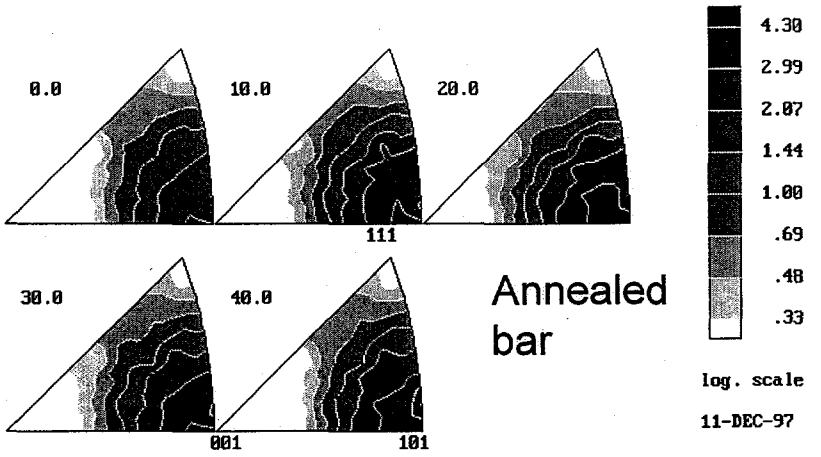

Figure 3. Same texture as Figures 1 and 2 (prestrain=0.5) assuming orthotropic sample symmetry for cubic crystal symmetry, represented as polar oblique sections assuming of 3-D orientation space, showing deviation from true fiber symmetry. The projection is the inverse pole figure for the normal direction. Sections plotted every 10° as oblique ν sections where ν is defined by the linear relationship $\nu=(\psi-\phi)/2$ in symmetric (Kocks) Euler angles. Plotted in multiples of random distribution (m.r.d.). (a) cold-worked, (b) annealed.

Normally the texture attains the same symmetry as the imposed strain tensor, but often the symmetry of the starting texture may be superimposed. In this study it is very likely an initial recrystallization texture was imposed on the deformation textures. Recrystllization inevitably occurs in most materials processing. Looking at the pole

figures of the annealed starting material in detail (plotted on a more revealing log scale plot, Figure 4) we see that indeed the annealed strain material posses a starting recrystallization texture.

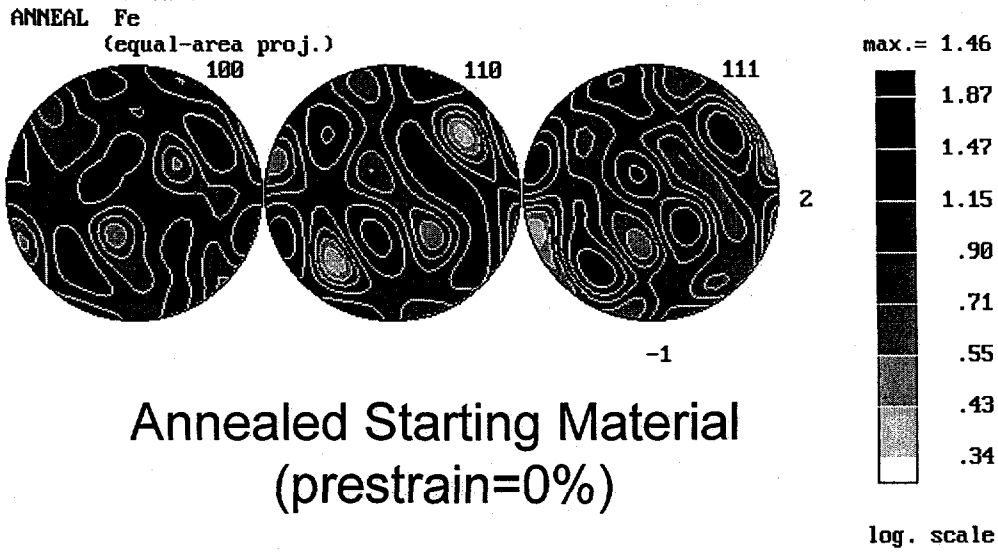

Figure 4. Pole figures of annealed starting material showing recrystallization starting texture. Plotted in equal area projection in multiples of random distribution (m.r.d.) on a log scale.

We do observe a decrease in the flow stress and work hardening rate in the 304L steel samples at room temperature at large strains. This observation is consistent with the samples approaching its saturation stress; a balance between defect storage and dynamic recovery processes. The saturation stress is strain rate and temperature dependent due to the suppression of dynamic recovery processes with decreasing temperature and/or increasing strain rate due to the decreased available thermal activation.

Both isotropic and anisotropic microstrains were calculated from the refinements used in the above pole figure studies. When samples experience macrostrains such as upset forging in this study, often the strains can vary continuously across the specimen causing peak locations for a particular hkl to shift slightly from spectrum to spectrum. The two microstrain parameters calculated here by Rietveld refinement are representative of a mean shift of all hkl's, although admittedly using mean values is a very crude description of the true anisotropic behavior of the residual strains [12]. Figure 5 shows a comparison of isotropic and anisotropic microstrains between cold worked (solid symbols) and annealed (open symbols) bars as a function of prestrain. Microstrains (μs) are plotted as a function of polar angle (χ) angle where 0° = parallel and 90° = perpendicular to compression.

Isotropic strains are constant with prestrain while anisotropic strains increase from approximately 5000 μs at ε=0.5 to 13000 at ε=1.8 μs parallel to the compression direction independent of whether the pre-forged starting material was in a cold worked or annealed condition. The positive and negative signs in these data refer to the sense of stress

relaxation left after pre-strain, where a positive sign is due to a tensile stress and a negative sign is due to a compressive stress. Isotropic strains remain in tension across the samples. Anisotropic strains change gradually, from compression (χ=0°) to tension (χ=90°) with slopes that increases with increasing prestrain. In the case of annealed material the data are notably scattered at ε=0.5 and the mean value rather than the compression intercept value is considered. Annealed bars that undergo reduced hardening rate at high strain have lower residual stress.

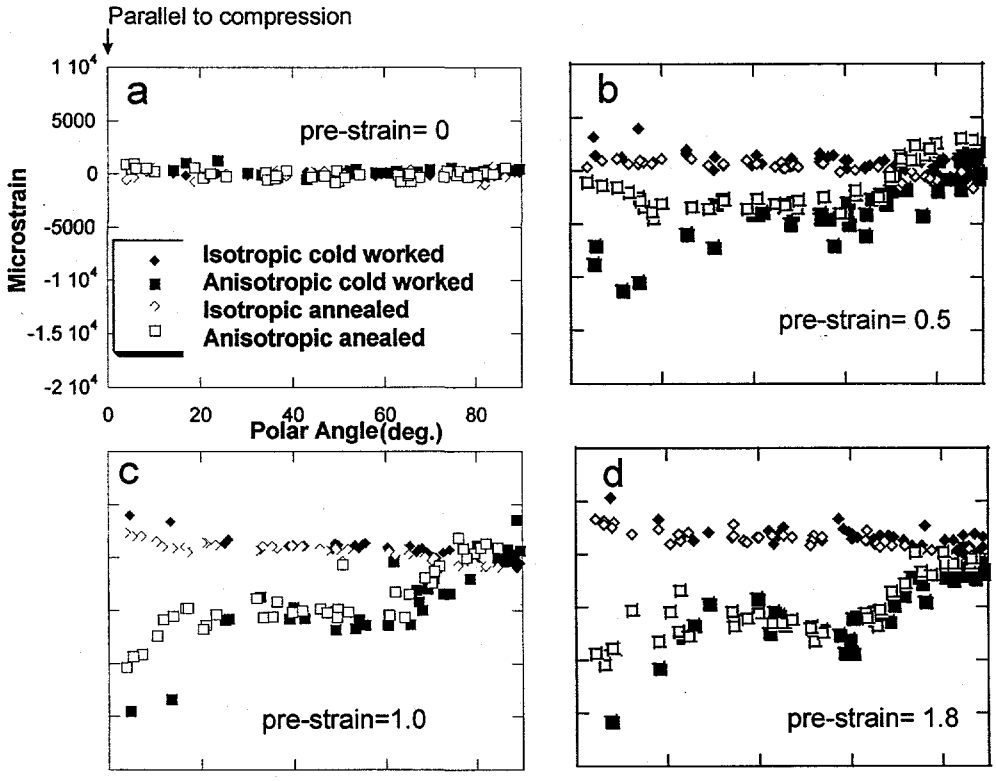

Figure 5. Calculated isotropic and anisotropic microstrains as a function of prestrain. Microstrain (μs) versus polar angle (degrees). 0° = parallel and 90° = perpendicular compression. Negative μs is compressive, positive μs is tensile.

Mechanical Results and Discussion

The compressive stress-strain responses of the 304L stainless steel under quasi-static and dynamic loading at strain rates (.001s^{-1}, .1s^{-1} and 2000s^{-1}) and temperatures (25°C and 77 K) are shown in Figure 6a (cold worked) and 6b (annealed) as a function of pre-strain. Both the cold worked and annealed 304L steel stress/strain curves show yield stresses that increase as a function of pre-strain. They also reveal that the yield stresses decreased by about a factor of 2 for an equivalent pre-strain when the samples were annealed compared to the cold-worked starting condition. The annealed curves demonstrate a reduced rate of

work hardening especially at higher pre-strains (1.0 and 1.8) though low temperature deformation (77 K) increases these rates again by about a factor of 4 (Figure 6b). The yield strength of these low temperature samples increases dramatically (approximately 70%) at quasi-static strain rate (0.001 s^{-1}). Conversely the yield strength is seen to increase only slightly for the cold-worked starting material (approximately 40%) even though strain rate is increased nearly 6 orders of magnitude. This observation is consistent with the attainment of a similar saturation stress (~ 1700 MPa) at room temperature for quasi-static loading of the cold-worked as well as the annealed preforged 304L material conditions. At room temperature the yield strength of the annealed material increases only slightly with a change in strain rates from $0.001s^{-1}$ to $0.1s^{-1}$ for all prestrains (Figure 6b). These observations are very consistent with established yield stresses in 304L austenitic stainless steel [15].

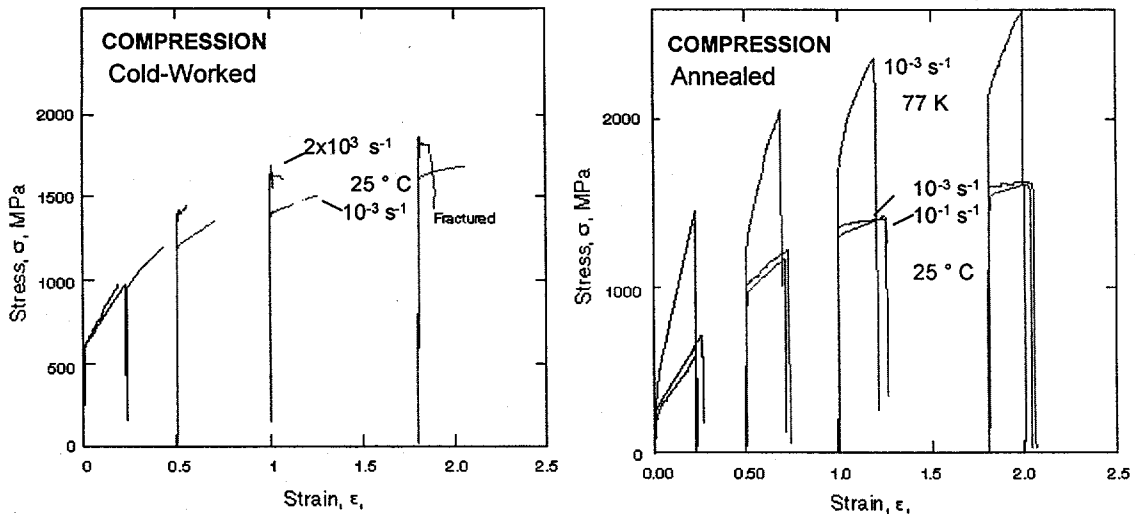

a b

Figure 6. Compressive stress/strain curves for the cold-worked 304L steel (a) and annealed (b) bars measured under quasi-static and dynamic load as a function of pre-strain ($.001s^{-1}$, 0.1 s^{-1} and $2000s^{-1}$) and temperature T=25°C at 77K. Only unloading portions of data for the annealed starting materials is shown.

Conclusions

304L stainless steel stock bar develops cyclic fiber texture with <110> fiber axis when upset-forged to large plastic strains independent of whether the 304L was forged in a cold-worked or annealed microstructural condition. For both 304L microstructural conditions the texture evolution for each (~3.0 m.r.d.) is seen to be achieved following a true strain of 0.5. The annealed 304L steel possessed a starting yield strength which was 50% that of the cold-worked 304L material for a fixed chemistry. At 77K the annealed 304L is seen to exhibit a 70% higher flow stress than at 298K in addition to a significantly higher work-hardening rate. This study documents the important relationship between texture and plasticity in polycrystalline metals and alloys. The development of advanced physically-based material models must integrate

crystallographic orientation effects on metal plasticity in addition to temperature and strain rate if predictive code capability is to be achieved.

Acknowledgments

We thankfully acknowledge United States Department of Energy, Office of Basic Energy Sciences- Materials Science, under contract number W-7405-ENG-36 with the University of California. The author KB acknowledges the assistance of R.W. Carpenter II for conducting the high-strain rate mechanical testing and M. F. Lopez for preparing the optical microscopy samples and conducting the quasi-static testing. The author KB acknowledges the assistance of Dr. V. A. Sukhoparov during her stay in Russia.

References

[1] P. S. Follansbee in Metals Handbook (1985, 9th Ed) 8, 198-302.
[2] H. M. Rietveld in The Rietveld Method (1995), R. A. Young Ed., 39-43.
[3] L. Lutterotti, S. Matthies and H.-R. Wenk, J. Appl. Phys. (1997) 81, 594-600.
[4] S. Matthies, L. Lutterotti and H. -R. Wenk, J. Appl. Cryst. (1997) 30, 31-42.
[5] R. B. Von Dreele J. Appl. Cryst.(1997). 30, 517-525
[6] B. N. Brockhouse, Can. J. Phys. (1953) 31, 339-355.
[7] G. T. Gray III in Methods in Materials Research (1997)(in press) John Wiley Press, New York.
[8] J. A. Robert MRS Bulletin (1997) 22, 42-46.
[9] U. F .Kocks, J. S. Kallend, H. -R. Wenk, A. D. Rollett and S. I. Wright POPLA: Preferred Orientation Package-Los Alamos (1995) LA-CC-89-18.
[10] S. Matthies Aktuelle Probleme der Texturanalyse (1982) Akad Wiss, D. D. R. Zentralinstitut fur Kernforschung, Rossendorf-Dresden.
[11] A. C. Larson and R. B. Von Dreele A GSAS Manual for Users (1994) LAUR 86-748.
[12] M. R. Daymond, M. A. M. Bourke, R. B. Von Dreele, B. Clausen, T. Lorentzen, J. Appl. Phys. (1997) 82, 1554-1562.
[13] M. G. Stout and P. S. Follansbee J. Eng. Mats. and Tech. (1986) 108, 344-353.
[14] H. Mecking in Preferred Orientation in Deformed Metals and Rocks: An Introduction to Modern Texture Analysis (1985) H. -R. Wenk ed., 267-302.
[15] C. Barrett and T. B. Massalski, Structure of Metals (1980, 3rd Ed.) McGraw-Hill, New York.